Acta Biochim Biophys Sin 2023, 55(11): 1806–1818
https://doi.org/10.3724/abbs.2023124
Advance Access Publication Date: 31 August 2023
Original Article

Original Article

Methyl cinnamate protects against dextran sulfate sodium-induced colitis in mice by inhibiting the MAPK signaling pathway

Lilin E[1,†], Wenjie Li[2,†], Yuanjia Hu[3], Lijuan Deng[4], Jianping Yao[2,*], and Xingwang Zhou[1,*]

[1]Department of Biochemistry and Molecular Biology, Sun Yat-sen University Zhongshan School of Medicine, Sun Yat-sen University, Guangzhou 510080, China, [2]The First Affiliated Hospital, Sun Yat-Sen University, Guangzhou 510080, China, [3]State Key Laboratory of Quality Research in Chinese Medicine, Institute of Chinese Medical Sciences, University of Macau, Macao SAR 999078, China, and [4]Formula-Pattern Research Center, School of Traditional Chinese Medicine, Jinan University, Guangzhou 510632, China

[†]These authors contributed equally to this work

*Correspondence address. Tel: +86-20-87332038; E-mail: zhouxw2@mail.sysu.edu.cn (X.Z.) / E-mail: yaojianp@mail.sysu.edu.cn (J.Y.)

Received 15 March 2023 Accepted 19 May 2023

Abstract

Effective and non-toxic therapeutic agents are lacking for the prevention and treatment of colitis. Previous studies found that methyl cinnamate (MC), extracted from galangal (*Alpinia officinarum* Hance), has anti-inflammatory properties. However, whether MC is effective as anti-colitis therapy remains unknown. In this study, we investigate the therapeutic effects of MC on dextran sulfate sodium (DSS)-induced colitis in mice and further explore its potential mechanism of action. MC treatment relieves symptoms associated with DSS-induced colitis, including the recovery of DSS-induced weight loss, decreases the disease activity index score, and increases the colon length without toxic side effects. MC treatment protects the integrity of the intestinal barrier in mice with DSS-induced colitis and inhibits the overexpression of pro-inflammatory cytokines *in vivo* and *in vitro*. Moreover, the MAPK signaling pathway is found to be closely related to the treatment with MC of colitis. Western blot analysis show that phosphorylation of the p38 protein in colon tissues treated with MC is markedly reduced and phosphorylation levels of the p38, JNK and ERK proteins are significantly decreased in RAW 264.7 cells treated with MC, indicating that the mechanism of MC in treating DSS-induced colitis could be achieved by inhibiting the MAPK signaling pathway. Furthermore, 16S RNA sequencing analysis show that MC can improve intestinal microbial dysbiosis in mice with DSS-induced colitis. Altogether, these findings suggest that MC may be a novel therapeutic candidate with anti-colitis efficacy. Furthermore, MC treatment relieves the symptoms of colitis by inhibiting the MAPK signaling pathway and improving the intestinal microbiota.

Key words methyl cinnamate, dextran sodium sulfate, inflammatory bowel disease, MAPK signaling pathway

Introduction

Inflammatory bowel disease (IBD) is an intestinal inflammatory disease with complex etiology and pathogenesis. IBD mainly includes Crohn's disease (CD) and Ulcerative colitis (UC) [1]. UC is a nonspecific inflammatory disease of the bowel characterized by a pattern of inflammation that typically begins in the rectum and extends proximally in a continuous fashion, eventually affecting part or all of the colonic mucosa [2]. In the last few decades, the incidence of UC has been increasing around the world [3]. Common clinical symptoms of UC include persistent bloody diarrhea, abdominal cramps, and fecal urgency, accompanied by the weight loss and fatigue [4,5], resulting in a severe decline in the quality of life of patients. In addition, patients with severe UC have a higher risk of developing colorectal cancer [6]. Therefore, UC has become a major intestinal disease that is endangering public health in modern society. Although multiple factors, such as genetic and environmental factors, impair the intestinal epithelial barrier, immune response dysfunction, inflammatory response, and intestinal flora dysbiosis are believed to be associated with UC [7,8]. Nonetheless, the etiology and specific pathogenesis of UC are still not fully

understood. Currently available drugs for the treatment of UC include 5-aminosalicylic acid, sulfasalazine, corticosteroids and immunosuppressants [9–11]. However, the clinical efficacy of these drugs is not satisfactory. For example, many drugs exhibit limited efficacy and have the potential to cause serious side effects such as nephrotoxicity and bone marrow suppression [12,13]. Additionally, there are no preventive medications available for UC. Therefore, there is an urgent need to develop new, safer and more effective therapies for the treatment of UC.

Alpinia officinarum Hance, belongs to the ginger family (Zingiberaceae), commonly called lesser galangal. The rhizomes of *A. officinarum* (galangal), named Gao-liang-jiang in Chinese, have received a great deal of attention for their potential applications in food and traditional Chinese medicine. Studies have shown that galangal exerts various biological activities that include anti-inflammatory, antibacterial, antioxidant and gastric protection [14,15]. Therefore, it has been used traditionally to treat gastrointestinal diseases such as stomachache, dyspepsia, and gastrofrigid vomiting [14,15]. Galangal contains a variety of bioactive ingredients with different pharmacological and medicinal properties, including flavonoids, diarylheptanoids and essential oils [16]. Among these compounds, galangin is the main flavonoid which possesses anti-inflammatory and anti-oxidant activities [16] and also exerts a protective effect on dextran sulfate sodium (DSS)-induced colitis in mice [17,18]. Methyl cinnamate (MC), the main component of the essential oil derived from galangal, has anti-inflammatory activity [19]. However, whether MC is effective in treating colitis in mice has not been reported so far.

In this study, the anti-inflammatory effects of MC on UC were evaluated *in vivo* and *in vitro* using a DSS-induced colitis mouse model, LPS-stimulated RAW264.7 cells and peritoneal elucidated macrophages (PEMs), respectively. The results suggest that MC could be a new therapeutic candidate derived from natural products for the treatment of UC.

Materials and Methods

Chemical Reagents

The compound MC (purity > 99%, verified by highperformance liquid chromatography) was obtained from Shanghai Yuanye Biotechnology Co., Ltd (Shanghai, China). DSS (molecular weight 36–50 kDa) and sulfasalazine (SASP) were purchased from Sigma-Aldrich (St Louis, USA).

Animal experiment

Female C57BL/6 mice (6–8 weeks old; $n = 40$) were purchased from the Guangdong Medical Laboratory Animal Center. All animal experiments were conducted according to protocols accredited by the Institutional Animal Care and Use Committee of Sun Yat-sen University for animal welfare (Guangzhou, China) (SYSU-IACUC-2020-000283). All mice were housed in a specific pathogen free animal room at a temperature of 24 ± 1°C and a humidity of 50%–70%. The rooms were under automatic lighting with a 12-h on–off cycle. Forty mice were randomly divided into the following five groups, with eight mice in each group: control, DSS, MC (20 mg/kg or 40 mg/kg) and SASP. All mice were treated orally. From the first to the seventh day, mice in the control group were given free access to pure drinking water, whereas those in the other groups were given access to 3% (w/v) DSS drinking water. The pure water and the DSS drinking water were changed every 2 days. From the first day to the 14th day, mice in the control and DSS groups received normal saline; the mice in the MC groups received 20 mg/kg or 40 mg/kg MC; the mice in the SASP-treated group received 50 mg/kg SASP. On day 14, the end of treatment, the body weight change, disease activity index (DAI) score and colon length of the mice were measured.

Evaluation of disease activity index

To evaluate the severity of colitis, body weight, fecal traits, and rectal bleeding were measured every day during the experiment period. The DAI is a quantitative index that is used to access the severity of colitis damage [20]. The DAI scores are defined as follows [21]: weight loss: 0 (no loss), 1 (1%–5% loss), 2 (5%–10% loss), 3 (10%–20% loss), and 4 (> 20% loss); stool consistency: 0 (normal), 2 (loose stool), and 4 (watery diarrhea); and hematochezia: 0 (no blood), 1 (Hemoccult positive), 2 (Hemoccult positive and visual pellet bleeding), and 4 (gross bleeding, blood around the anus). DAI scores were determined daily during the experiment.

Histological analysis

After the mice were euthanized, small segments of distal colon samples and other main organs (*e.g.*, heart, liver, spleen, lung and kidney) were collected and the colon length of each mouse was measured. The mice colon tissues and the main organs of mice were then washed with cold PBS. Part of the colon tissues and the organs were fixed with 4% paraformaldehyde for 24 h at room temperature and then embedded in paraffin. All the samples were cut into 4-μm-thick sections and stained with hematoxylin and eosin (H&E) for morphological analysis. H&E stained colonic tissue sections were scored by a blinded observer using a previously published system [21].

Immunohistochemistry analysis

For immunohistochemistry (IHC) analysis of tight junction (TJ) proteins such as ZO-1, colon tissues were excised, weighed and fixed in 4% neutral paraformaldehyde solution, embedded in paraffin, and sectioned. The sections were then dewaxed and hydrated. Endogenous peroxidase activity was blocked with a solution of 3% H_2O_2 after antigen retrieval. After wash with PBS (pH 7.4) for 15 min, the sections were blocked with 5% bovine serum albumin (BSA) in PBS at 37°C for 30 min. Next, the sections were incubated overnight at 4°C with anti-ZO-1 antibody (Abcam, Cambridge, UK). After being washed, sections were incubated with the secondary antibody at room temperature for 30 min. The sections were then stained with diaminobenzidine (DAB) for 5 min. The sections were counterstained with hematoxylin, dehydrated, mounted with neutral resin, and finally photographed. Images were taken on an Olympus BX61 microscope (Olympus, Tokyo, Japan) with a DP73 camera. Quantitative analysis of target proteins were performed using ImageJ 1.5.7 (NIH, Bethesda, USA).

Cell culture

The mouse macrophage cell line RAW264.7 was obtained from the American Type Culture Collection (ATCC, Manassas, USA). Peritoneal elucidated macrophages (PEMs) were collected from mice treated with an i.p. injection of 3% Brewer thioglycollate medium. These cells were cultured in high glucose DMEM medium (HyClone, Logan, USA) supplemented with 10% FBS (Sigma, St

Louis, USA) and 1% penicillin-streptomycin (HyClone) at 37°C in a humidified incubator with a CO_2 atmosphere of 5%. RAW264.7 cells and PEMs were stimulated with 1 μg/mL LPS (Sigma), followed by treatment with different concentrations of MC.

Cell viability assay

The impact of MC treatment on cell viability was assessed by CCK-8 assay. RAW 264.7 cells and PEMs were seeded in 96-well plates at a density of 7×10^3 cells/well and cultured overnight. When cell density reached 60%–70%, cells were treated with different concentrations of MC (6.25, 12.5, 25, 50, 75 and 100 μM) for 24 h. Five parallel wells were set for each group, 10 μL of CCK-8 solution was added to each well. The 96-well plate was then incubated in the incubator for at least 1 h. A microplate reader was used to evaluate the absorbance at 450 nm.

Measurement of pro-inflammatory cytokine production

The cellular and tissue levels of the inflammatory cytokines TNF-α, IL-1β and IL-6 were detected by enzyme-linked immunosorbent assay (ELISA). Briefly, the colon tissues of the mice were washed, homogenized, and then centrifuged at 10,000 *g* for 20 min at 4°C. The supernatants were collected and the levels of TNF-α, IL-1β, and IL-6 were detected using the corresponding ELISA kits (Invitrogen, Carlsbad, USA) according to the procedure recommended by the supplier. Furthermore, RAW 264.7 cells and PEMs were seeded in 6-well plates at a density of 1.2×10^6 cells/well. The cells were then co-treated with different concentrations of MC (25, 50, and 100 μM) with 1 μg/mL LPS for 24 h. The levels of inflammatory cytokines TNF-α, IL-1β and IL-6 in the cell culture medium were measured in the same way.

Western blot analysis

Total proteins from colon tissues and RAW264.7 cells were extracted using RIPA buffer containing protease and phosphatase inhibitor cocktails. The total protein concentration was determined using a BCA protein assay kit (Beyotime Biotech, Shanghai, China). Aliquots containing 40 μg of total protein were separated by 10% sodium dodecylsulphate-polyacrylamide gel electrophoresis (SDS-PAGE) and transferred to a polyvinylidene difluoride (PVDF) membrane. The membrane was blocked with 5% BSA for 1 h at room temperature and then incubated with the indicated primary antibodies at 4°C overnight. Subsequently, the membranes were incubated with the indicated HRP-conjugated secondary antibodies (CST, Danvers, USA) at room temperature for 1 h. Finally, the protein bands were detected with the western blot substrate (Gene Tech, Shanghai, China) and images were obtained using the GE Image Quant Las4000mini (GE Healthcare, Chicago, USA). The primary antibodies used for the investigation were as follows: P38 (CST), p-P38 (CST), ERK1/2 (CST), p-ERK1/2 (CST), JNK1/2 (CST), p-JNK1/2 (Promega, Madison, USA) and GAPDH (Abmart, Shanghai, China).

Bioinformatics analysis

The structure of MC was acquired from the PubChem database (https://pubchem.ncbi.nlm.nih.gov/) and its potential targets were selected by the Swiss Target Prediction Database (http://www.swisstargetprediction.ch/). The key word "ulcerative colitis" was used to query the Genecards database (http://www.genecards.org) to obtain the potential targets for the treatment of UC. Then, common targets of MC and UC were used to construct the PPI network using the STRING database (https://string-db.org/) and Cytoscape 3.9.1 software. According to the centrality of a node and the number of its neighbor nodes [22], the core genes in the PPI network were evaluated using R v3.6. To study the potential signaling pathway triggered by MC for the treatment of UC, the Visualization and Integrated Discovery (DAVID) database (https://david.ncifcrf.gov/) was used to interrogate the Kyoto Encyclopedia of Genes and Genomes (KEGG) pathways. The results were visualized using an online bioinformatics platform (http://www.bioinformatics.com.cn/).

16S RNA sequencing analysis

Fecal samples were frozen immediately after collection and stored in a freezer at –80°C for subsequent experiments. High-throughput 16S RNA sequencing of the fecal samples was performed at Panomic Biomedical Technology Co., Ltd (Suzhou, China). Total bacterial DNA was extracted from fecal samples using the OMEGA Soil DNA Kit (OMEGA, Norcross, USA) following the manufacturer's instructions. PCR amplification of the region of the 16S bacterial RNA genes V3-V4 was performed using the forward primer 338F (5′-ACTCCTACGGGAGGCAGCAA-3′) and the reverse primer 806R (5′-GGACTACHVGGGTWTCTAAT-3′). After purification and quantification of the PCR products, the sequencing library was built. Finally, the library was sequenced on the Illumina NovaSeq platform (Illumina, San Diego, USA).

Microbiome bioinformatics analysis was performed using QIIME2 and R packages v3.2.0. Valid sequences were merged using QIIME2 software, and sequences with ≥97% similarity were classified into the same operational taxonomic units (OTUs). Representative sequences for each OTU were screened for further analysis. A representative sequence of OTUs was annotated and taxonomically analyzed using the GREENGENES 13.8 database. The diversity of samples and the differences of microbial community structure among samples were investigated by taxonomic composition analysis, the Alpha diversity analysis, and the Beta diversity analysis.

Statistical analysis

Unless otherwise stated, all experiments were repeated three times, and data were expressed as the mean ± SD. GraphPad Prism 8 was used for statistical analysis. Histological analyses were performed in a blinded manner. The DAI score, body weight change and CCK8 assay results were analyzed by two-way ANOVA; other experimental data were compared using one-way ANOVA and unpaired two-tailed Student's *t*-test. A value of $P < 0.05$ was considered statistically significant.

Results

MC improved the pathological symptoms of DSS-induced colitis in mice

The DSS-induced colitis model was used to evaluate the therapeutic effects of MC (structure shown in Figure 1A) on UC in mice (Figure 1B). Compared to the DSS group mice, the body weight of MC- and SASP-treated mice was greater (Figure 1C). Specifically, the body weight of mice treated with high-concentration MC (40 mg/kg) increased significantly, the body weight of mice treated with low-concentrations of MC (20 mg/kg) and SASP increased slightly. In addition, all DAI scores increased in DSS-, MC- and SASP-treated mice compared to that in the control group mice. However, the

increase in DAI in the DSS group was most notable. MC administration reversed the increase in DAI induced by DSS in a dose-dependent manner (Figure 1D). Similarly, the colon length of the mice in DSS group was significantly shortened compared to that in the control group mice. However, MC administration reversed this shortening when the oral dose was increased (Figure 1E). In particular, when compared to the SASP treatment (positive control), the higher concentration MC treatment (40 mg/kg) more effectively relieved the pathological symptoms of DSS-induced colitis (Figure 1C–E). We also evaluated the toxicity of MC in mice. There were no obvious histopathological damages in the main organs (such as heart, liver, spleen, lung and kidney) of the mice after MC treatment (Supplementary Figure S1). Altogether, these results indicated that MC relieved symptoms of DSS-induced colitis in a dose-dependent manner, suggesting that MC had a protective effect on DSS-induced colitis in mice.

MC preserved the integrity of the intestinal barrier of DSS-induced colitis in mice

The histopathological characteristics of DSS colitis in mice reflects

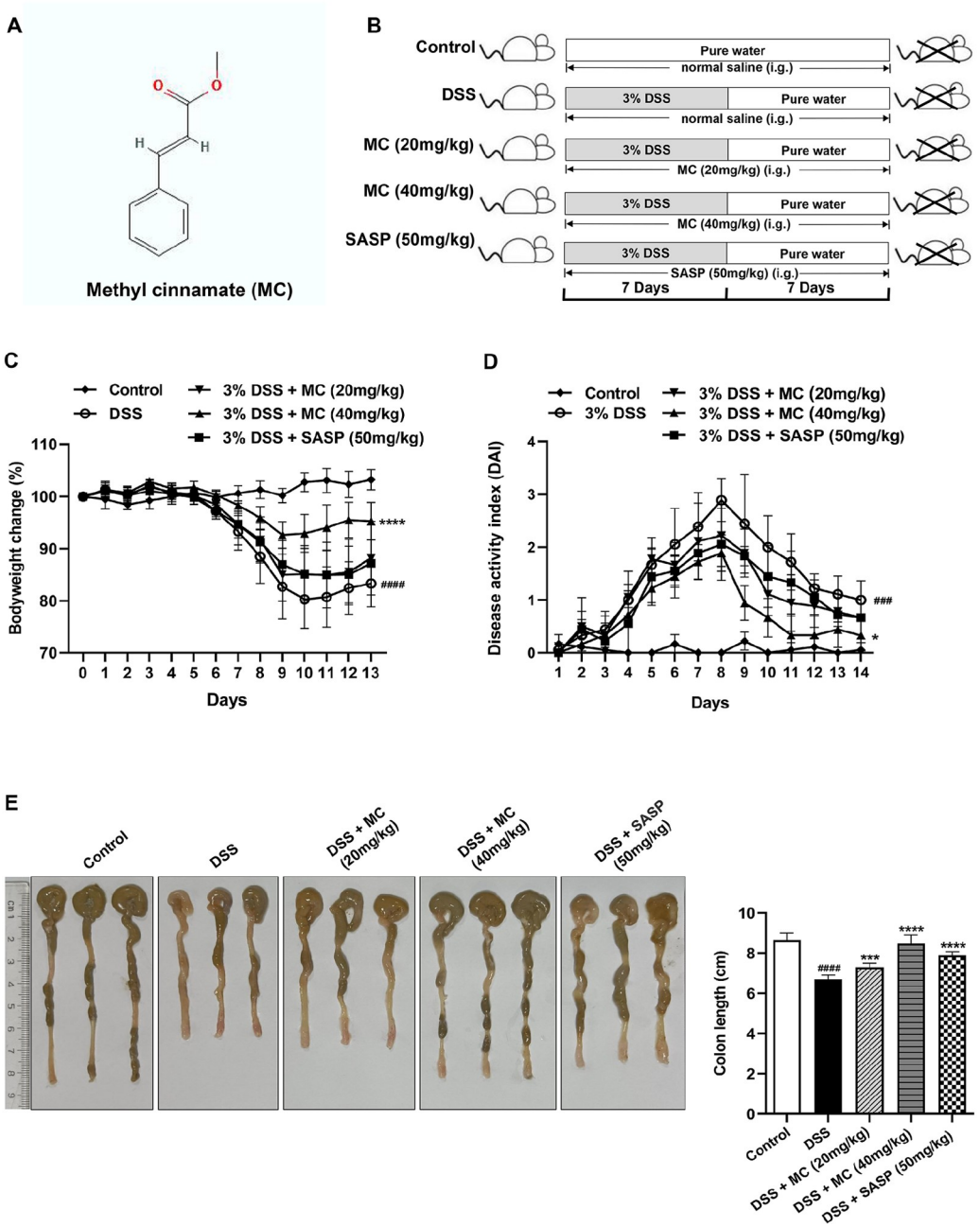

Figure 1. MC alleviates symptoms of DSS-induced colitis in mice (A) Molecular structure of MC. (B) Schematic diagram of the *in vivo* experimental design. (C) Body weight of mice recorded during the experiment. (D) DAI of mice was recorded daily during the experimental period. (E) Images and statistical results of colon length. Data are presented as the mean ± SD ($n = 6$ per group). ###$P < 0.001$, ####$P < 0.0001$ compared to the control group. *$P < 0.05$, ***$P < 0.001$, ****$P < 0.0001$, compared to the DSS group.

those seen in human IBD, which include mainly the disappearance of colonocytes, the reduction of goblet cells and crypts, and the infiltration of inflammatory cells in the mucosa [23]. Therefore, to further evaluate the effects of MC treatment on the pathological improvement of colonic inflammation and ulceration, H&E staining was used to access pathological changes of colonic tissues.

As shown in Figure 2A, the cross-section of the colon in normal mice consisted of the mucosa, submucosa, muscularis, and serosa layers from the inside to the outside. The control group showed a healthy colon with an intact mucosal epithelial structure and natural intestinal mucosal folds, tall columnar surface colonocytes, and a large number of goblet cells and crypts. While the mucosa layer in the colons of DSS-treated mice was destroyed, numerous crypts, colonocytes and goblet cells disappeared, and a large number of inflammatory cells infiltrated into the mucosa and submucosa. However, the histological damage of colon tissue in the DSS-induced colitis model was alleviated after MC and SASP treatment (Figure 2A). Specifically, the colon structure of mice treated with MC was intact; colonocytes, goblet cells, and crypts in the colon increased and mucosal inflammatory cell infiltration was significantly reduced, indicating that MC had a good therapeutic effect. Consequently, the histological score of the DSS group was significantly higher than that of the control group, and the histological score of the MC and SASP treatment was significantly lower than that of the DSS group (Figure 2B). These results indicated that MC prevented DSS-induced tissue damage and

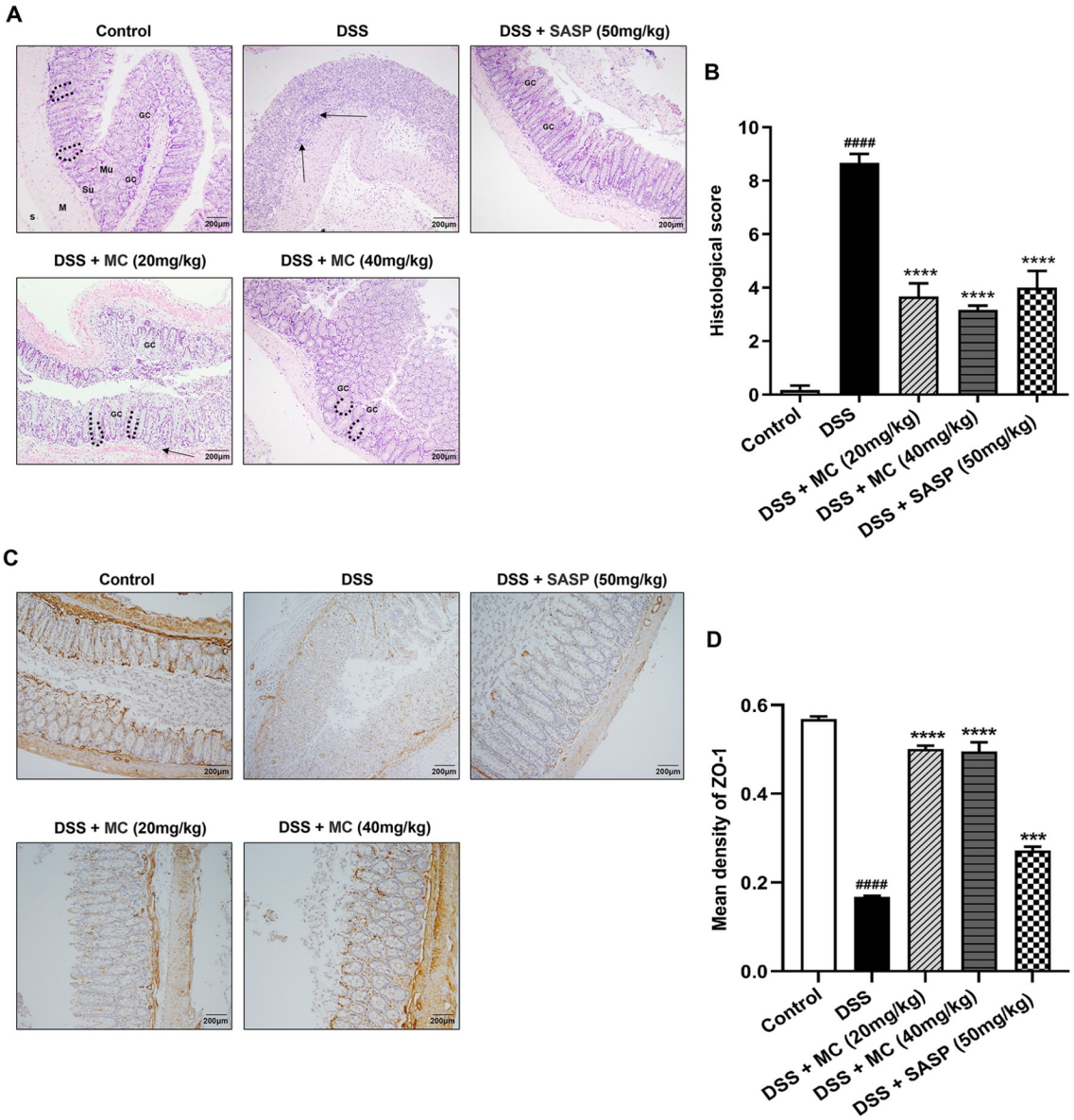

Figure 2. MC preserves intestinal barrier integrity of dextran sulfate sodium-induced colitis in mice (A) Representative histological images of the colon stained by H&E (magnification, × 100), scale bar: 200 μm; GC: goblet cells; Mu: mucosa; Su: submucosa; M: muscle; S: serosa; Black dotted line highlights crypts, black arrow indicates the infiltration of inflammatory cells. (B) Histological scores of colon tissues in A. (C) Representative immunostaining images of the colon for ZO-1 (magnification, × 100), scale bar: 200 μm. (D) Bar graphs of the mean density of ZO-1 in C. Data are presented as the mean ± SEM from three independent experiments. $^{\#\#\#\#}P < 0.0001$ compared to the control group. $^{***}P < 0.001$, $^{****}P < 0.0001$ compared to the DSS group.

exerted potent protective effects against DSS-induced colitis.

Recent studies have reported that a loss of barrier integrity can exacerbate intestinal inflammation [24], and that the integrity of the epithelial barrier is mainly maintained by TJ proteins such as ZO-1 [25,26]. Therefore, we evaluated the effects of MC treatment on ZO-1 expression in the mouse colon using IHC (Figure 2C,D). The IHC results showed that ZO-1 was highly expressed and well-organized in the colon tissue of normal mouse (control). As expected, DSS treatment greatly reduced the expression of ZO-1 protein, while MC treatment effectively suppressed these changes. After MC treatment, the expression of ZO-1 was almost completely restored compared to the control group, and was more obvious than that of the SASP group. These results indicate that the protective effects of MC against DSS-induced colitis were related to the maintenance of the epithelial barrier and that MC treatment protected the integrity of the intestinal barrier of DSS-induced colitis in mice.

MC inhibited pro-inflammatory cytokine production in the colon of DSS-treated mice

Pro-inflammatory cytokines (TNF-α, IL-1β and IL-6) play an important role in the pathogenesis of IBD [27]. Here, we examined the expression of these pro-inflammatory cytokines in mouse colon tissue using ELISA. As shown in Figure 3A–C, compared to the control group, the production of TNF-α, IL-1β and IL-6 increased significantly in the DSS group. In contrast, TNF-α, IL-1β, and IL-6 levels were significantly decreased in the groups treated with MC and SASP compared to the DSS group. These results indicate that MC treatment could attenuate inflammation in mouse DSS-induced colitis by inhibiting pro-inflammatory cytokines.

MC downregulated pro-inflammatory cytokine production in RAW 264.7 cells and PEMs. We examined the effects of MC treatment on RAW 264.7 cells to confirm its anti-inflammatory effects *in vitro*. First, we performed the CCK-8 assay to evaluate the effects of MC treatment on the cell viability of RAW 264.7 cells and PEMs. The results showed that MC was nontoxic across the dose range 6.25–100 μM (Figure 4A). We then detected the production of pro-inflammatory cytokines (TNF-α, IL-1β and IL-6) in cell culture supernatants of RAW264.7 cells and PEMs by ELISA. Compared to the control group, the production of TNF-α, IL-1β and IL-6 increased significantly after LPS treatment (Figure 4B–G). In contrast, the production of TNF-α, IL-1β, and IL-6 in the MC treatment cell culture supernatant markedly decreased compared to the LPS group in a dose-dependent manner (Figure 4B–G). These results demonstrated that MC treatment alleviated LPS-induced inflammation *in vitro*.

Network pharmacology predicted the key targets and potential signaling pathways for MC treatment of UC

To explore the mechanism of action of MC in the treatment of colitis, a network pharmacology analysis was performed to screen potential effector targets of MC in colitis. The intersection analysis using the Draw Venn diagrams online tool showed that there were 24 overlapping target proteins in total between MC and colitis (Figure 5A). Next, the protein–protein interaction (PPI) network of 24 overlapping targets was analyzed using String (Figure 5B). By summing up the edge numbers of a node, we obtained the centrality of 23 target genes, of which mitogen-activated protein kinase (MAPK)14 and MAPK8 had 11 and 12 neighboring genes respectively. MAPK14 was identified as the core gene involved in the pathogenesis of colitis (Figure 5C). Furthermore, the KEGG analysis performed using the DAVID database identified the top 30 enriched signaling pathways (Figure 5D), which included the MAPK signaling pathway. These results indicate that MC treats colitis through multiple pathways and multiple targets, and the MAPK signaling pathway could be closely related to the treatment of colitis by MC.

MC inhibited the MAPK signaling pathway in the mouse colitis model and in RAW264.7 cells

The results of network pharmacology analysis (Figure 5) revealed that the MAPK signaling pathway could be related to the underlying mechanism of MC in the treatment of colitis. To test this hypothesis, the levels of total and phosphorylated proteins involved in the MAPK signaling pathway, including p38, JNK and ERK proteins, were detected by western blot analysis in mouse colon tissues and RAW 264.7 cells.

As shown in Figure 6A,B, compared to the control group, the phosphorylation of the p38 protein in the colon tissue of the DSS-treated group of mice was significantly increased. Conversely, compared to the DSS group, treatment with MC at the dose of 40 mg/kg significantly reduced the expression of phosphorylated p38 protein, which was also similar to the SASP group. Additionally, in RAW 264.7 cells, the LPS-induced group showed an increase in the phosphorylation of the p38, JNK and ERK proteins compared to the control group (Figure 6C,D). Compared to the LPS-induced group, MC treatment at doses of 25, 50 and 100 μM decreased the

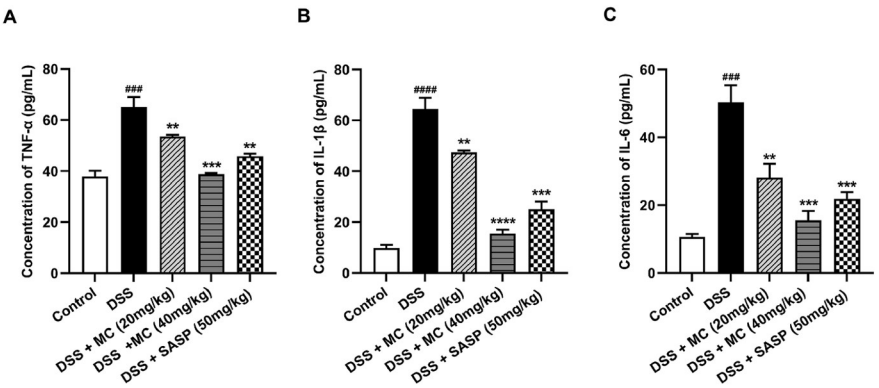

Figure 3. MC inhibits pro-inflammatory cytokines in colonic tissues Fourteen days after treatment, the colonic tissues were collected and the production of TNF-α (A), IL-1β (B) and IL-6 (C) were determined by ELISA. Data presented as the mean ± SEM from three independent experiments ($n = 6$ per group). $^{###}P < 0.001$, $^{####}P < 0.0001$ compared to the control group. $^{**}P < 0.01$, $^{***}P < 0.001$, $^{****}P < 0.0001$ compared to the DSS group.

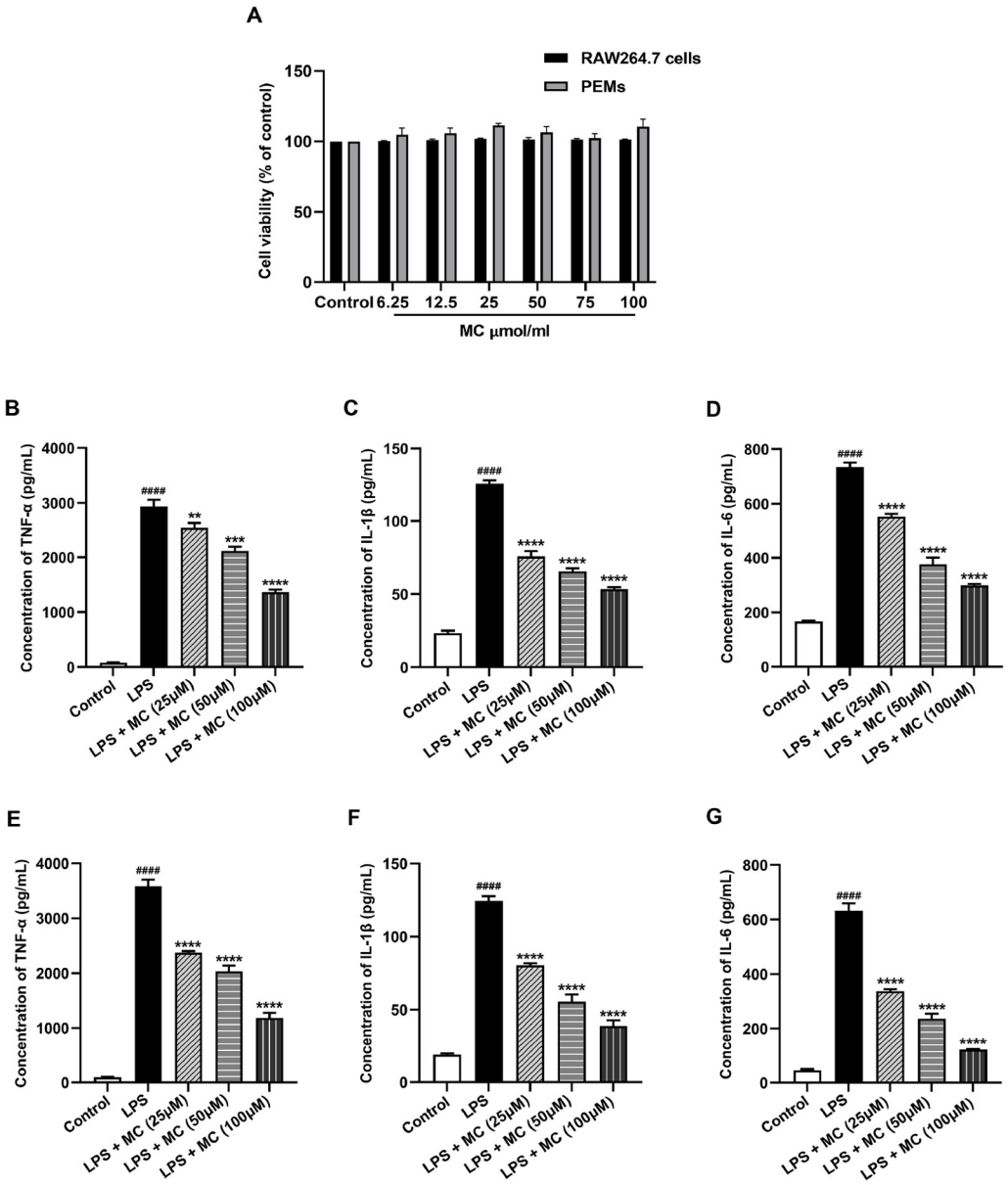

Figure 4. MC downregulates LPS-induced pro-inflammatory cytokine production by RAW264.7 cells and PEMs (A) The impact of MC treatment (6.25, 12.5, 25, 50, 75 and 100 μM) on RAW264.7 cell and PEMs viability was determined. RAW264.7 cells and PEMs were pretreated with different concentrations of MC for 24 h. Cell viability of treated cells were determined by the CCK8 assay. Data are presented as the mean ± SD from three independent experiments. (B–D) LPS-stimulated RAW264.7 cell culture supernatants were collected and the levels of TNF-α (B), IL-1β (C) and IL-6 (D) were determined by ELISA. (E–G) LPS-stimulated PEMs culture supernatants were collected and the levels of TNF-α (E), IL-1β (F) and IL-6 (G) were determined by ELISA. Data are presented as the mean ± SEM from three independent experiments (n = 6 per group). $^{\#\#\#\#}P < 0.0001$ compared to the control group. $^{**}P < 0.01$, $^{***}P < 0.001$, $^{****}P < 0.0001$ compared to the LPS group.

phosphorylation of p38, JNK, and ERK proteins, among which the 100 μM dose decreased phosphorylation levels the most significantly (Figure 6C,D). These results suggest that MC treatment could attenuate inflammatory responses to colitis *in vivo* and *in vitro* by inhibiting the MAPK signaling pathway.

MC improved the intestinal microbiota in mice with DSS-induced colitis

Previous report has shown that IBD is associated with compositional changes in the intestinal microbiota [28]. We further evaluated the changes in the intestinal microbiota after MC treatment of DSS-induced colitis in mice using 16S RNA sequencing analysis.

Species accumulation curves showed that there were more than 4000 species of intestinal microorganisms in the three groups (control, DSS, and MC treated a dose of 40 mg/kg), which essentially represented the more common species (Figure 7A). When comparing the common intestinal microbiota among different groups using a Venn diagram, there were 778 overlapping OTUs (7.5%) among three groups, 243 overlapping OTUs (2.34%)

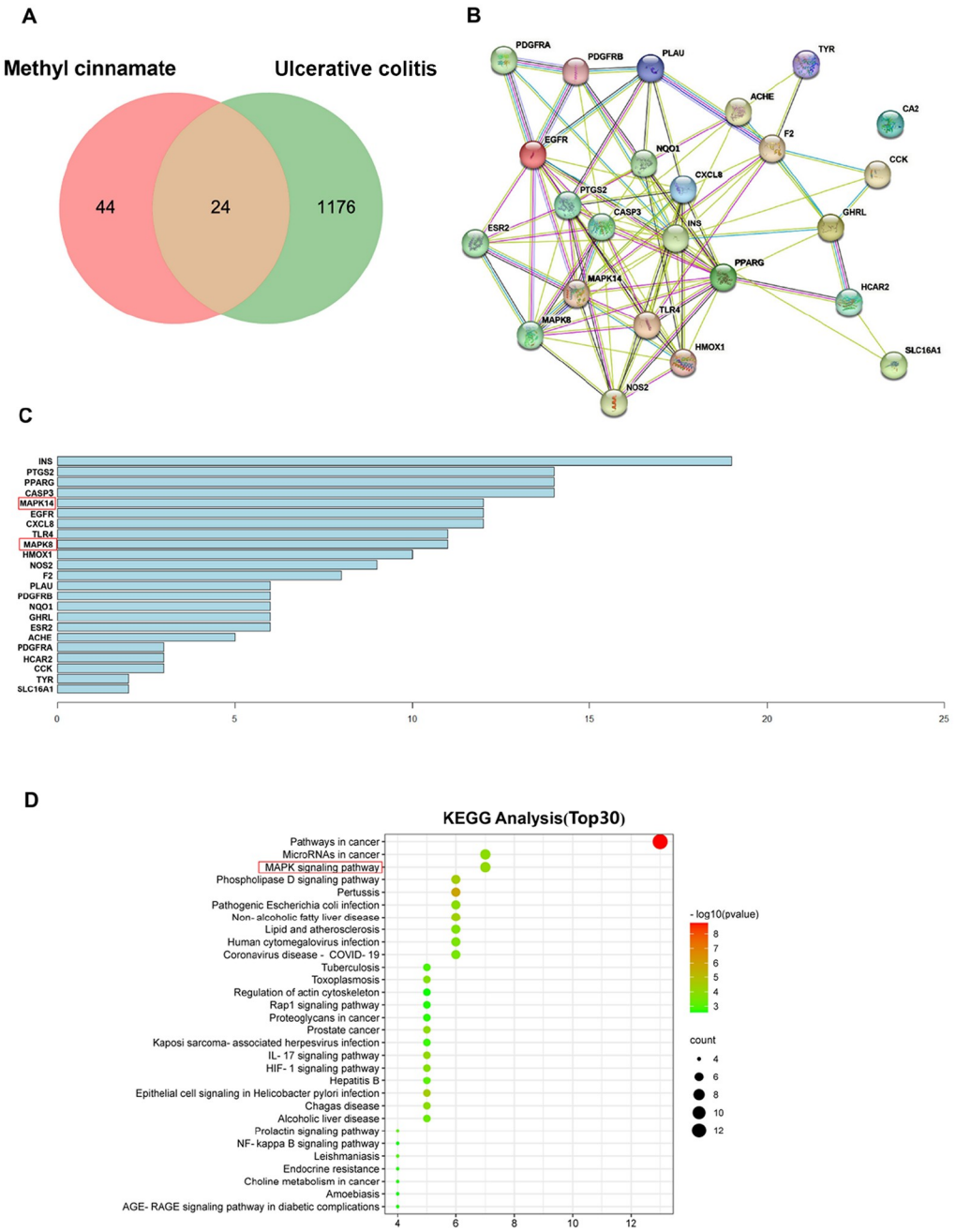

Figure 5. Network pharmacology prediction of MC treatment for DSS-induced colitis (A) Venn diagram depicting the intersection of the targets of MC and colitis. Twenty-four overlapping targets of MC acting on UC. (B) The result of protein-protein interaction (PPI) network analysis for the potential targets of MC. (C) Summing up the edge numbers of a node to predict core genes in PPI network. Core genes in PPI network ranked by nodal centrality. (D) KEGG analysis for the potential enriched signaling pathways of the common target genes. Count number≥30.

between the control group and the DSS group, 386 overlapping OTUs (3.72%) between the DSS group and the MC group, and 370 overlapping OTUs (3.57%) between the control group and the MC group (Figure 7B). The Rank abundance curve at the species level showed that the intestinal microbiota abundance was the highest in the control group and the lowest in the DSS group, and the MC group was midway between the control and DSS groups (Figure 7C). As shown in the heat map of cluster analysis at the genus level in Figure 7D, the microbiota composition of the control and DSS groups was markedly separated, while that of the MC group was close to the composition of the control group. The principal component analysis (PCA) and the principal coordinate analysis (PCoA) showed that the distribution of intestinal microbiota in the control and DSS groups was well separated, while that of the MC and control groups was closely clustered (Figure 7E).

A difference in intestinal microbiota composition was observed in the three test groups and controls (at the phylum and genus levels) after cluster analysis (Figure 7F,G). At the phylum level (Figure 7F),

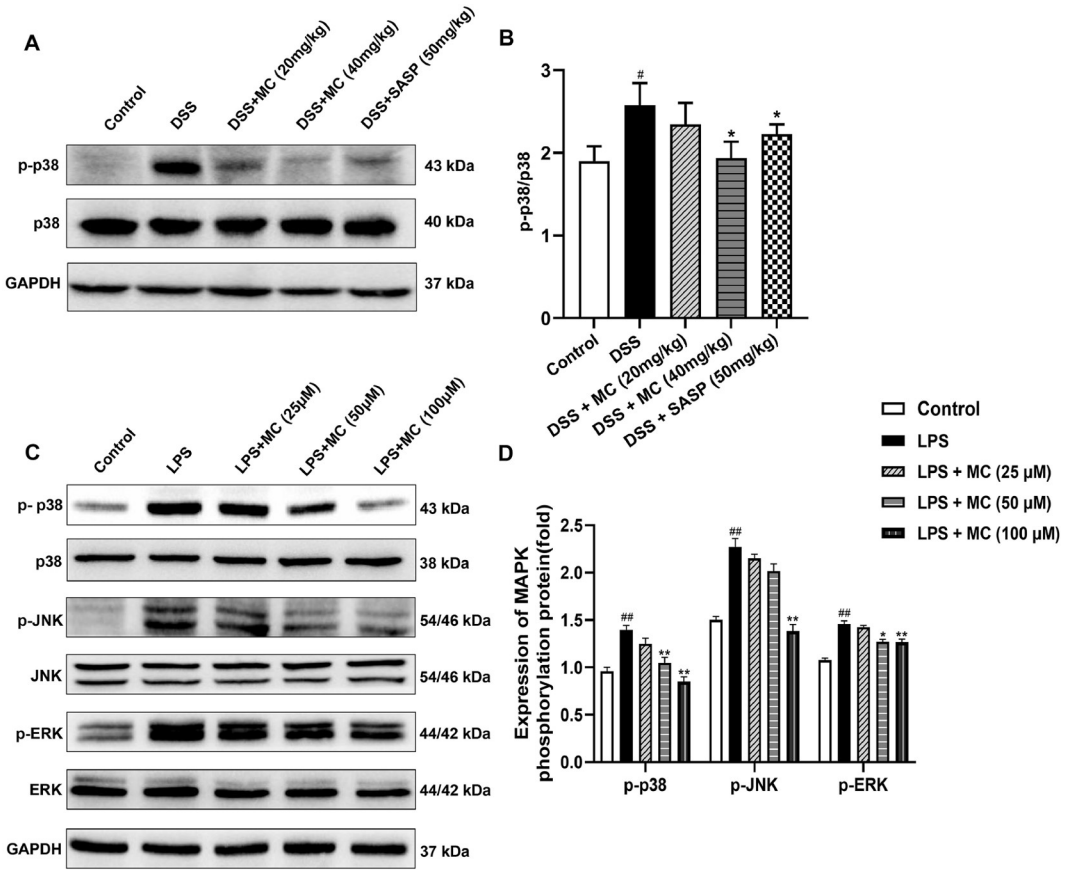

Figure 6. Effects of MC on the MAPK signaling pathway *in vivo* and *in vitro* (A,B) Effects of MC on the expressions of key proteins in the MAPK signaling pathway in colonic tissues of mice. Fourteen days after treatment, the colonic tissues were collected and p38 and p-p38 protein expressions in the colonic tissues were detected by western blot analysis. Data are presented as the mean ± SEM from three independent experiments ($n = 6$ per group). $^{\#}P < 0.05$ compared to the control group. $^{*}P < 0.05$ compared to the DSS group. (C,D) Effects of MC on expression levels of key proteins in the MAPK signaling pathway in RAW264.7 cells. RAW264.7 cells were treated with different concentrations of MC (25 μM, 50 μM, and 100 μM) and LPS (1 μg/mL) for 24 h. The expressions of key proteins of the MAPK pathway (p-p38, p38, p-JNK, JNK, p-ERK, and ERK) in treated RAW264.7 cells were detected by western blot analysis. Data are presented as the mean ± SEM from three independent experiments ($n = 6$ per group). $^{\#\#}P < 0.01$ compared to the control group. $^{*}P < 0.05$, $^{**}P < 0.01$ compared to the LPS-treated group.

Bacteroidetes and *Firmicutes* acted as dominant species in all three groups. Compared to the control group, the abundance of *Firmicutes* decreased significantly and that of *Bacteroidetes* and *Proteobacteria* increased markedly in the DSS group. However, there was a significant increase in the abundance of *Firmicutes* and *Verrucomicrobia* and a decrease in the abundance of *Bacteroidetes* and *Proteobacteria* after administration of MC compared to the DSS group. Furthermore, at the genus level (Figure 7G), the intestinal microbiota in all three groups were mainly composed of *Lactobacillus*, *Akkermansia*, *Bacteroides* and *Allobaculum*. Specifically, compared to the control group, the abundance of *Bacteroides* increased significantly in the DSS group, while the abundance of *Bacteroides* markedly decreased after the administration of MC. The abundance of *Lactobacillus* and *Akkermansia* in the MC group increased significantly compared to the DSS group. Studies have shown that *Bacteroidetes* exhibit pro-inflammatory properties that contribute to IBD [29], suggesting that *Bacteroidetes* could be pathogenic bacteria. Whereas *Akkermansia* and *Lactobacillus* are generally recognized as probiotics [30]. Overall, a significant decrease in the abundance of pathogenic bacteria and an increase in the abundance of probiotic bacteria could be observed in the MC group compared to those in the DSS group. These results suggest that MC treatment improves the intestinal microbiota of mice with DSS-induced colitis.

Discussion

UC is a human IBD of unknown etiology, characterized mainly by intestinal inflammation and mucosal damage [2]. The current clinical treatment of UC mainly includes corticosteroids, aminosalicylates, sulfonamides, and immunosuppressive agents, but these drugs usually have serious side effects, which limit their clinical application [31,32]. Therefore, there is an urgent need to develop novel ingredients that have good preventive and therapeutic effects on UC with less side effects. Natural products may act as a good source of new therapeutic candidates for UC. Galangal is a traditional Chinese herb with "homology of medicine and food" that can be used to treat various gastrointestinal diseases [16]. However, the bioactive ingredients of galangal still need to be further validated. MC, the main essential oil of galangal, has been reported to have anti-inflammatory activity but has not been studied in the treatment of colitis [19]. Here, we report for the first time the protective effects of MC on DSS-induced colitis in mice. The results

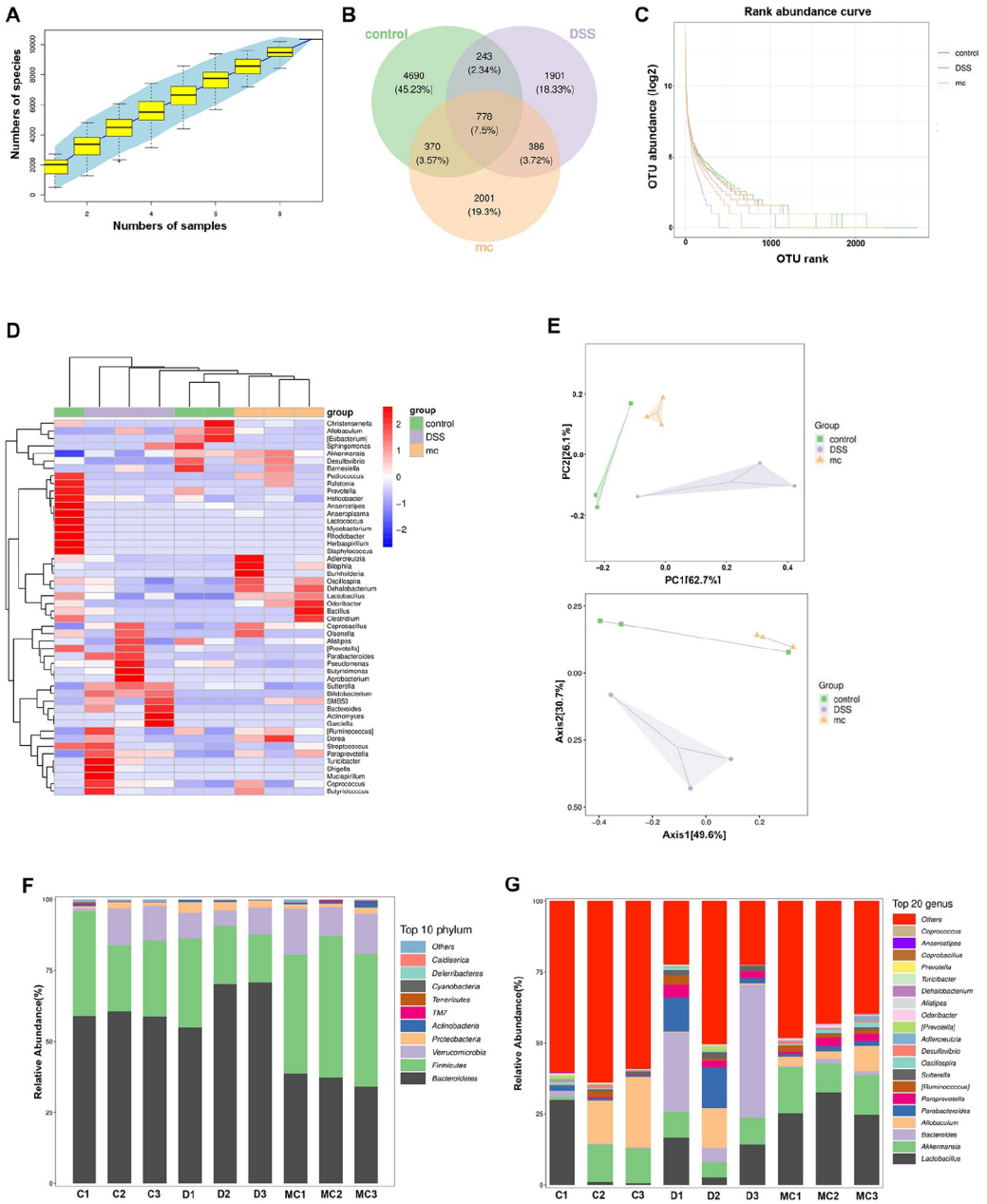

Figure 7. MC improves the intestinal microbiota of dextran sulfate sodium-induced colitis in mice (A) Sample number and species richness were estimated from the Species accumulation curves. (B) Venn diagram display of common or endemic species in three groups through the numbers of OTUs. (C) Rank abundance curve of species level. (D) Heatmap showing the relative abundance of intestinal microbiota at the genus level. C1 (control group 1), C2 (control 2), C3 (control 3); D1 (DSS group 1), D2 (DSS 2), D3 (DSS 3); methyl cinnamate (MC). (E) PCA and PCoA indicated distinct structural changes in the overall bacterial community of each group. Each plot represents one sample. (F) The column chart of the relative distribution of each group at the phylum level, showing the top 10 phyla in colon samples from three groups. (G) The column chart of the relative distribution of each group at the genus level, showing the top 20 genera in colon samples from three groups.

revealed that MC treatment markedly relieved symptoms associated with DSS-induced colitis.

The main features of severe colitis include epithelial erosions and ulcers, crypt abscesses, goblet cell depletion, loss of the mucus layer, and massive neutrophil infiltration of the lamina propria, which can be assessed by histopathological observation and histological scores [33]. In the present study, we found that MC treatment greatly restored DSS-induced mucosal layer disruption and attenuated the loss of columnar colonocytes, goblet cells and crypts. Additionally, the infiltration of inflammatory cells in the mucosa and submucosa was also significantly reduced. Thus, MC has the ability to alleviate the symptoms of DSS-induced colitis in mice.

The intestinal barrier is composed of a mechanical, chemical, immune, and microbial barrier. It is well known that breakdown of intestinal barrier function is closely related to the occurrence and development of IBD [34], while the integrity of the intestinal epithelial barrier is mainly associated with TJs [24]. TJs are mainly composed of TJ proteins; abnormal expression of TJ proteins such

as ZO-1 in intestinal tissue can change intestinal permeability and increase pathogen infiltration, which eventually leads to an excessive immune response and induces IBD [35,36]. As such, we also detected the expressions of TJ proteins in intestinal tissues of DSS colitis in mice after MC treatment. We found that DSS treatment significantly decreased the expression of ZO-1 protein in mouse intestinal tissues, while MC treatment significantly reversed this phenotypic change. The results indicate that MC treatment could help restore the integrity of the intestinal barrier in the DSS-induced colitis mouse model.

Increasing evidence has shown that pro-inflammatory cytokines play a critical role in the pathogenesis of UC and are directly related to the severity, duration, and complications of IBD [18,37]. Overexpression of pro-inflammatory cytokines TNF-α, IL-6 and IL-1β can cause intestinal inflammation and intestinal dysfunction [38,39]. Therefore, inhibiting the excessive increase in pro-inflammatory cytokines could be an effective therapeutic approach to treat UC. In clinical treatment, monoclonal antibody drugs, including adalimumab (TNF-α mAb) and tocilizumab (IL-6 mAb) have been shown to be effective in the treatment of UC patients [40]. In addition, IL-1β has been identified as a potential target for clinical intervention in UC patients who do not respond to TNF-α antibody neutralization [41]. In this study, we found that MC significantly reduced the overexpression of TNF-α, IL-1β, IL-6 in mouse colon tissue. Moreover, MC also inhibited the overexpression of TNF-α, IL-1β, IL-6 in LPS-induced RAW264.7 cells, PEMs (Figure 4) and human THP-1 cells (Supplementary Figure S2). However, the anti-inflammatory efficacy of MC on THP-1 cells was relatively weak compared to that on RAW264.7 cells and PEMs. All these data suggest that MC could exert anti-inflammatory effects on DSS-induced colitis in mice.

Network pharmacology targets biological networks and analyzes the connections among drugs, targets, and diseases in these networks. As an emerging discipline based on the theory of systems biology, network pharmacology has been widely used to study the targets of drugs or human diseases [42,43]. The network pharmacology approach used in this study showed that MAPK14 could be a core gene associated with the pathogenesis of colitis. The p38α protein encoded by the MAPK14 gene is one of the key targets of the MAPK signaling pathway [44]. KEGG analysis also indicated that the MAPK signaling pathway could be closely related to the treatment of colitis by MC (Figure 5D).

In mammals, MAPK is an intracellular serine/threonine (Ser/Thr) kinase that plays an important role in various cellular functions such as migration, proliferation, differentiation, growth and inflammation [45,46]. It has been shown that MAPK is a key regulator of IBD. After activation of the MAPK signaling pathway, the transcription and expression of different inflammatory molecules related to IBD are also altered, exacerbating the development of intestinal inflammation [47]. The MAPK pathway is a highly conserved signaling pathway. p38 MAPK, extracellular signal-regulated protein kinase (ERK) and c-Jun N-terminal kinase (JNK) are considered the main kinases of the MAPK pathway, which can be induced by various cytokines and hormones [48]. Current studies have shown that the activity of p38 MAPK increases in patients with IBD [49], and the activation of p38 MAPK promotes the secretion of pro-inflammatory cytokines such as TNF-α and IL-1β, thereby mediating the inflammatory response [50]. Meanwhile, JNK and ERK activation could also regulate the secretion of pro-inflammatory cytokines such as TNF-α and IL-6, thus affecting the inflammatory response [51,52]. In this study, we found that MAPK signaling was significantly altered in DSS-induced mouse colitis after MC treatment. That is, the phosphorylation level of p38 protein was markedly decreased in colon tissues treated with MC, and the phosphorylation levels of p38, JNK and ERK proteins were significantly decreased in RAW 264.7 cells treated with MC (Figure 6). Previous studies also reported that other natural products such as flavaglines, fisetin, myricitrin, and cardamonin possess therapeutic effects against IBD via modulation of different segments of the MAPK signaling pathway, suggesting that targeting the MAPK pathway may be a promising direction for the discovery of new anti-colitis therapies [47].

The intestinal microbiota has coevolved with humans, and various symbiotic interactions between them are essential for maintaining human health. Dysbiosis caused by adverse changes in the composition and function of the intestinal microbiota can cause or exacerbate a range of human diseases [53]. In IBD, intestinal flora dysbiosis can alter the intestinal microenvironment and disrupt the intestinal epithelial barrier, making the intestinal mucosa more susceptible to invasion by pathogenic bacteria [54]. It was reported that increasing the abundance of *Firmicutes* and decreasing the abundance of *Bacteroides* and *Proteobacteria* using fecal microbiota transplantation can alleviate DSS-induced colitis in mice [55]. Furthermore, the abundance of *Verrucomicrobia*, *Akkermansia* and *Lactobacillus* are markedly increased following drug treatment in a DSS-induced mouse model [56]. In this study, we found that MC treatment could significantly increase the abundance of *Firmicutes* and *Verrucomicrobia* but decrease the abundance of the *Bacteroidetes* and *Proteobacteria* at the phylum level. Moreover, at the genus level, MC treatment markedly reduced the abundance of *Bacteroides* and increased the abundance of beneficial bacteria, including *Lactobacillus* and *Akkermansia*. Overall, the results of intestinal flora analysis in this study are basically consistent with the relevant literature reports, indicating that MC treatment could ameliorate intestinal microbial dysbiosis in colitis.

In conclusion, we report for the first time that MC, as the main essential oil ingredient in galangal, has a significant protective effect on DSS-induced colitis. Oral administration of MC to mice effectively relieves symptoms of DSS-induced colitis in mice. Furthermore, the toxicity test (Supplementary Figure S1) show that MC, which is derived from natural herbal plants of the same origin of medicine and food, has good safety during treatment. On the other hand, although the mouse model of acute colitis in this study is a classic model used to study enteritis, we intend to further validate the therapeutic effect of MC on enteritis in the future using the chronic colitis model as well as clinical samples, considering that chronic colitis is more common in patients. Overall, our study suggests that MC could be a novel therapeutic candidate for the treatment of colitis.

Supplementary Data

Supplementary data is available at *Acta Biochimica et Biophysica Sinica* online.

Acknowledgement

We would like to thank Dr. Ce Tang (The First Affiliated Hospital, Sun Yat-sen University) and Dr. Dinghong WU (The Second Clinical Medical College, Guangzhou University of Chinese

Medicine) for their helpful discussion and comments. We also thank Miss. Qianyao Ren and Mr. Dingli Zhou of Sun Yatsen University for their technical assistance.

Funding

This work was supported by the grants from the Guangdong Basic and Applied Basic Research Foundation (No. 2019B1515120051) and the National Natural Science Foundation of China (No. 82174022).

Conflict of Interest

The authors declare that they have no conflict of interest.

References

1. Mao R, Hu PJ. The future of IBD therapy: where are we and where should we go next? *Dig Dis* 2016, 34: 175–179
2. Ferretti F, Cannatelli R, Monico MC, Maconi G, Ardizzone S. An update on current pharmacotherapeutic options for the treatment of ulcerative colitis. *J Clin Med* 2022, 11: 2302
3. Ng SC, Shi HY, Hamidi N, Underwood FE, Tang W, Benchimol EI, Panaccione R, *et al.* Worldwide incidence and prevalence of inflammatory bowel disease in the 21st century: a systematic review of population-based studies. *Lancet* 2017, 390: 2769–2778
4. Ryan FJ, Ahern AM, Fitzgerald RS, Laserna-Mendieta EJ, Power EM, Clooney AG, O'Donoghue KW, *et al.* Colonic microbiota is associated with inflammation and host epigenomic alterations in inflammatory bowel disease. *Nat Commun* 2020, 11: 1512
5. Ungaro R, Mehandru S, Allen PB, Peyrin-Biroulet L, Colombel JF. Ulcerative Colitis. *Lancet* 2017, 10080: 1756–1770
6. Lasry A, Zinger A, Ben-Neriah Y. Inflammatory networks underlying colorectal cancer. *Nat Immunol* 2016, 17: 230–240
7. Ananthakrishnan AN. Epidemiology and risk factors for IBD. *Nat Rev Gastroenterol Hepatol* 2015, 12: 205–217
8. Harris KG, Chang EB. The intestinal microbiota in the pathogenesis of inflammatory bowel diseases: new insights into complex disease. *Clin Sci* 2018, 132: 2013–2028
9. Ge H, Cai Z, Chai J, Liu J, Liu B, Yu Y, Liu J, *et al.* Egg white peptides ameliorate dextran sulfate sodium-induced acute colitis symptoms by inhibiting the production of pro-inflammatory cytokines and modulation of gut microbiota composition. *Food Chem* 2021, 360: 129981
10. Chen P, Xu H, Tang H, Zhao F, Yang C, Kwok L, Cong C, *et al.* Modulation of gut mucosal microbiota as a mechanism of probiotics-based adjunctive therapy for ulcerative colitis. *Microb Biotechnol* 2020, 13: 2032–2043
11. Levesque BG, Sandborn WJ, Ruel J, Feagan BG, Sands BE, Colombel JF. Converging goals of treatment of inflammatory bowel disease from clinical trials and practice. *Gastroenterology* 2015, 148: 37–51.e1
12. Da Silva S, Keita ÅV, Mohlin S, Påhlman S, Theodorou V, Påhlman I, Mattson JP, *et al.* A novel topical PPARγ agonist induces PPARγ activity in ulcerative colitis mucosa and prevents and reverses inflammation in induced colitis models. *Inflammatory Bowel Dis* 2018, 24: 792–805
13. Hindryckx P, Vande Casteele N, Novak G, Khanna R, D'Haens G, Sandborn WJ, Danese S, *et al.* The expanding therapeutic armamentarium for inflammatory bowel disease: how to choose the right drug[s] for our patients? *J Crohns Colitis* 2018, 12: 105–119
14. Namdeo AG, Kale VM. Comparative pharmacognostic and phytochemical investigation of two Alpinia species from Zingiberaceae Family. *World J Pharm Res* 2015, 4: 1417–1432
15. Abubakar IB, Malami I, Yahaya Y, Sule SM. A review on the ethnomedicinal uses, phytochemistry and pharmacology of Alpinia officinarum Hance. *J Ethnopharmacol* 2018, 224: 45–62
16. Zhou YQ, Liu H, He MX, Wang R, Zeng QQ, Wang Y, Ye WC, *et al.* A review of the botany, phytochemical, and pharmacological properties of galangal. *Natural and Artificial Flavoring Agents and Food Dyes* 2018, 351–396
17. Sangaraju R, Nalban N, Alavala S, Rajendran V, Jerald MK, Sistla R. Protective effect of galangin against dextran sulfate sodium (DSS)-induced ulcerative colitis in Balb/c mice. *Inflamm Res* 2019, 68: 691–704
18. Xuan H, Ou A, Hao S, Shi J, Jin X. Galangin protects against symptoms of dextran sodium sulfate-induced acute colitis by activating autophagy and modulating the gut microbiota. *Nutrients* 2020, 12: 347
19. Murakami Y, Kawata A, Suzuki S, Fujisawa S. Cytotoxicity and Pro-/Anti-inflammatory properties of cinnamates, acrylates and methacrylates against RAW264.7 cells. *In Vivo* 2018, 32: 1309–1322
20. Wirtz S, Popp V, Kindermann M, Gerlach K, Weigmann B, Fichtner-Feigl S, Neurath MF. Chemically induced mouse models of acute and chronic intestinal inflammation. *Nat Protoc* 2017, 12: 1295–1309
21. Kim JJ, Shajib MS, Manocha MM, Khan WI. Investigating intestinal inflammation in DSS-induced model of IBD. *J Vis Exp* 2012, 60: 3678
22. Barabási AL, Oltvai ZN. Network biology: understanding the cell's functional organization. *Nat Rev Genet* 2004, 5: 101–113
23. Perše M, Cerar A. Dextran sodium sulphate colitis mouse model: traps and tricks. *J Biomed Biotechnol* 2012, 2012: 1–13
24. Capaldo CT, Powell DN, Kalman D. Layered defense: how mucus and tight junctions seal the intestinal barrier. *J Mol Med* 2017, 95: 927–934
25. Yuan J, Cheng W, Zhang G, Ma Q, Li X, Zhang B, Hu T, *et al.* Protective effects of iridoid glycosides on acute colitis via inhibition of the inflammatory response mediated by the STAT3/NF-κB pathway. *Int Immunopharmacol* 2020, 81: 106240
26. Li C, Wang M, Chen X, Chen W. Taraxasterol ameliorates dextran sodium sulfate-induced murine colitis via improving intestinal barrier and modulating gut microbiota dysbiosis. *Acta Biochim Biophys Sin* 2022, 54: 340–349
27. Zhu W, Ren L, Zhang L, Qiao Q, Farooq MZ, Xu Q. The potential of food protein-derived bioactive peptides against chronic intestinal inflammation. *Mediators Inflamm* 2020, 2020: 1–15
28. Ni J, Wu GD, Albenberg L, Tomov VT. Gut microbiota and IBD: causation or correlation? *Nat Rev Gastroenterol Hepatol* 2017, 14: 573–584
29. Stojanov S, Berlec A, Štrukelj B. The influence of probiotics on the firmicutes/Bacteroidetes ratio in the treatment of obesity and inflammatory bowel disease. *Microorganisms* 2020, 8: 1715
30. Singh TP, Natraj BH. Next-generation probiotics: a promising approach towards designing personalized medicine. *Crit Rev Microbiol* 2021, 47: 479–498
31. Weisshof R, El Jurdi K, Zmeter N, Rubin DT. Emerging therapies for inflammatory bowel disease. *Adv Ther* 2018, 35: 1746–1762
32. Zhu X, Sun Y, Zhang Y, Su X, Luo C, Alarifi S, Yang H. Dieckol alleviates dextran sulfate sodium-induced colitis via inhibition of inflammatory pathway and activation of Nrf2/HO-1 signaling pathway. *Environ Toxicol* 2021, 36: 782–788
33. Chassaing B, Aitken JD, Malleshappa M, Vijay-Kumar M. Dextran sulfate sodium (DSS)-induced colitis in mice. *CP Immunol* 2014, 104: 15.25
34. Zhang H, Wang Y, Su Y, Fang X, Guo W. The alleviating effect and mechanism of Bilobalide on ulcerative colitis. *Food Funct* 2021, 12: 6226–6239
35. Zeisel MB, Dhawan P, Baumert TF. Tight junction proteins in gastrointestinal and liver disease. *Gut* 2019, 68: 547–561
36. Weersma RK, Zhernakova A, Fu J. Interaction between drugs and the gut microbiome. *Gut* 2020, 69: 1510–1519
37. Xavier RJ, Podolsky DK. Unravelling the pathogenesis of inflammatory

bowel disease. *Nature* 2007, 448: 427–434
38. Neurath MF. Cytokines in inflammatory bowel disease. *Nat Rev Immunol* 2014, 14: 329–342
39. Zhang H, Hua R, Zhang B, Zhang X, Yang H, Zhou X. Serine alleviates dextran sulfate sodium-induced colitis and regulates the gut microbiota in mice. *Front Microbiol* 2018, 9: 3062
40. Sahu BD, Kumar JM, Sistla R. Fisetin, a dietary flavonoid, ameliorates experimental colitis in mice: relevance of NF-κB signaling. *J Nutral Biochem* 2016, 28: 171–182
41. De Santis S, Kunde D, Galleggiante V, Liso M, Scandiffio L, Serino G, Pinto A, ***et al.*** TNFα deficiency results in increased IL-1β in an early onset of spontaneous murine colitis. *Cell Death Dis* 2017, 8: e2993
42. Yuan H, Ma Q, Cui H, Liu G, Zhao X, Li W, Piao G. How can synergism of traditional medicines benefit from network pharmacology? *Molecules* 2017, 22: 1135
43. Li C, Wang M, Sui J, Zhou Y, Chen W. Protective mechanisms of Agrimonia pilosa Ledeb in dextran sodium sulfate-induced colitis as determined by a network pharmacology approach. *Acta Biochim Biophys Sin* 2021, 53: 1342–1353
44. Liang R, Chen W, Fan H, Chen X, Zhang J, Zhu JS. Dihydroartemisinin prevents dextran sodium sulphate-induced colitis through inhibition of the activation of NLRP3 inflammasome and p38 MAPK signaling. *Int Immunopharmacol* 2020, 88: 106949
45. Pearson G, Robinson F, Beers Gibson T, Xu B, Karandikar M, Berman K, Cobb MH. Mitogen-activated protein (MAP) kinase pathways: regulation and physiological functions. *Endocrine Rev* 2001, 22: 153–183
46. Cuadrado A, Nebreda AR. Mechanisms and functions of p38 MAPK signalling. *Biochem J* 2010, 429: 403–417
47. Zobeiri M, Momtaz S, Parvizi F, Tewari D, Farzaei MH, Nabavi SM. Targeting mitogen-activated protein kinases by natural products: a novel therapeutic approach for inflammatory bowel diseases. *Curr Pharm Biotechnol* 2020, 21: 1342–1353
48. Chang L, Karin M. Mammalian MAP kinase signalling cascades. *Nature* 2001, 410: 37–40
49. Hommes D, Van Den Blink B, Plasse T, Bartelsman J, Xu C, Macpherson B, Tytgat G, ***et al.*** Inhibition of stress-activated MAP kinases induces clinical improvement in moderate to severe Crohn's disease. *Gastroenterology* 2002, 122: 7–14
50. Feng YJ, Li YY. The role of p38 mitogen-activated protein kinase in the pathogenesis of inflammatory bowel disease. *J Digestive Dis* 2011, 12: 327–332
51. Kyriakis JM, Avruch J. Mammalian MAPK signal transduction pathways activated by stress and inflammation: a 10-year update. *Physiol Rev* 2012, 92: 689–737
52. Gao W, Wang C, Yu L, Sheng T, Wu Z, Wang X, Zhang D, ***et al.*** Chlorogenic acid attenuates dextran sodium sulfate-induced ulcerative colitis in mice through MAPK/ERK/JNK pathway. *Biomed Res Int* 2019, 2019: 1–13
53. Nishida A, Inoue R, Inatomi O, Bamba S, Naito Y, Andoh A. Gut microbiota in the pathogenesis of inflammatory bowel disease. *Clin J Gastroenterol* 2018, 11: 1–10
54. Grishin A, Bowling J, Bell B, Wang J, Ford HR. Roles of nitric oxide and intestinal microbiota in the pathogenesis of necrotizing enterocolitis. *J Pediatr Surg* 2016, 51: 13–17
55. Zhang W, Zou G, Li B, Du X, Sun Z, Sun Y, Jiang X. Fecal microbiota transplantation (FMT) alleviates experimental colitis in mice by gut microbiota regulation. *J Microbiol Biotechnol* 2020, 30: 1132–1141
56. Huang P, Wang X, Wang S, Wu Z, Zhou Z, Shao G, Ren C, ***et al.*** Treatment of inflammatory bowel disease: Potential effect of NMN on intestinal barrier and gut microbiota. *Curr Res Food Sci* 2022, 5: 1403–1411